Available online at www.sciencedirect.com
ScienceDirect
Journal of Solid State Chemistry 180 (2007) 2452–2458
JOURNAL OF SOLID STATE CHEMISTRY
www.elsevier.com/locate/jssc

Rare earth metal-rich indides $RE_{14}Rh_{3-x}In_3$ (RE = Y, Dy, Ho, Er, Tm, Lu)

Roman Zaremba, Rainer Pöttgen*

Institut für Anorganische und Analytische Chemie, Universität Münster, Corrensstrasse 30, D-48149 Münster, Germany

Received 14 March 2007; received in revised form 6 June 2007; accepted 10 June 2007
Available online 15 June 2007

Abstract

The rare earth (RE) metal-rich indides $RE_{14}Rh_{3-x}In_3$ (RE = Y, Dy, Ho, Er, Tm, Lu) can be synthesized from the elements by arc-melting or induction melting in tantalum crucibles. They were investigated by X-ray diffraction on powders and single crystals: $Lu_{14}Co_3In_3$ type, space group $P4_2/nmc$, $Z = 4$, $a = 961.7(1)$, $c = 2335.5(5)$ pm, w$R2 = 0.052$, 2047 F^2 values, 62 variables for $Y_{14}Rh_3In_3$, $a = 956.8(1)$, $c = 2322.5(5)$ pm, w$R2 = 0.068$, 1730 F^2 values, 63 variables for $Dy_{14}Rh_{2.89(1)}In_3$, $a = 952.4(1)$, $c = 2309.2(5)$ pm, w$R2 = 0.041$, 1706 F^2 values, 63 variables for $Ho_{14}Rh_{2.85(1)}In_3$, $a = 948.6(1)$, $c = 2302.8(5)$ pm, w$R2 = 0.053$, 1977 F^2 values, 63 variables for $Er_{14}Rh_{2.86(1)}In_3$, $a = 943.8(1)$, $c = 2291.5(5)$ pm, w$R2 = 0.065$, 1936 F^2 values, 63 variables for $Tm_{14}Rh_{2.89(1)}In_3$, and $a = 937.8(1)$, $c = 2276.5(5)$ pm, w$R2 = 0.050$, 1637 F^2 values, 63 variables for $Lu_{14}Rh_{2.74(1)}In_3$. Except $Yb_{14}Rh_3In_3$, the 8g Rh1 sites show small defects. Striking structural motifs are rhodium-centered trigonal prisms formed by the RE atoms with comparatively short Rh–RE distances (271–284 pm in $Y_{14}Rh_3In_3$). These prisms are condensed via common corners and edges building two-dimensional polyhedral units. Both crystallographically independent indium sites show distorted icosahedral coordination. The icosahedra around In2 are interpenetrating, leading to In2–In2 pairs (309 pm in $Y_{14}Rh_3In_3$).

Keywords: Indides; Intermetallics; Crystal chemistry

1. Introduction

The different rare earth (RE) metal-rich intermetallic $RE_xT_yIn_z$ compounds (T = late transition metal) show a common structural motif. The transition metal atoms as the most electronegative component fill trigonal prismatic or octahedral voids formed by the more electropositive RE metal atoms [1]. The striking structural units in the structure types $Lu_{14}Co_3In_3$ [2,3] and Gd_4RhIn [4] are two-, respectively three-dimensional networks of edge- and corner-sharing trigonal CoRE_6 and RhRE_6 prisms. These networks are relatively rigid with short Co–RE and Rh–RE distances. In the $Lu_{14}Co_3In_3$ type [2,3] the two-dimensional networks are separated by the polyhedra around the indium atoms, while cages within the three-dimensional network of the Gd_4RhIn type [4] are filled by In_4 tetrahedra and the polyhedra around the RE1 site that is not part of the trigonal prisms. In the $Ce_{12}Pt_7In$ type [5] structure, platinum-filled trigonal prisms occur besides square antiprisms.

Empty RE_6 octahedra occur in the structure types $Sm_{12}Ni_6In$ [6], Ho_6Co_2Ga [7], and $Er_{12}Fe_2In_3$ [8]. These octahedra are condensed via all common corners, leading to a ReO_3-related framework. The voids left by the octahedral frameworks are filled by indium atoms and T_2 dumb-bells.

A special situation is found for the RE metal-rich parts of the RE–Rh–In systems. Besides the series of Gd_4RhIn (i.e. $RE_{12}Rh_3In_3$) type indides, even RE-richer compounds $RE_{14}Rh_3In_3$ with $Lu_{14}Co_3In_3$ [2,3] exist. The synthesis and structure refinements of $RE_{14}Rh_3In_3$ (RE = Y, Dy, Ho, Er, Tm, Lu) are reported herein.

2. Experimental

2.1. Synthesis

Starting materials for the preparation of the $RE_{14}Rh_3In_3$ (RE = Y, Dy, Ho, Er, Tm, Lu) indides were ingots of the

*Corresponding author.Fax: +49 251 83 36002.
E-mail address: pottgen@uni-muenster.de (R. Pöttgen).

0022-4596/$ - see front matter © 2007 Elsevier Inc. All rights reserved.
doi:10.1016/j.jssc.2007.06.005

RE elements (Johnson Matthey, Chempur or Kelpin), rhodium granules (Heraeus), and indium tear drops (Merck), all with stated purities better than 99.9%. In a first step, the *RE* metal pieces were arc-melted [9] under 600 mbar argon to small buttons. The argon was purified over titanium sponge (900 K), silica gel, and molecular sieves. The pre-melting procedure reduces shattering during the subsequent reactions with rhodium and indium. The *RE* metal buttons were then mixed with pieces of the rhodium granules and the indium tear drops in the ideal 14:3:3 atomic ratios. The mixtures were reacted in the arc-furnace and remelted three times to ensure homogeneity. The weight losses after the arc-melting procedures were always smaller than 0.5%. The light gray polycrystalline samples are brittle and stable in air over months. Finely ground powders are dark gray and single crystals exhibit metallic luster.

Alternatively the samples can be prepared by induction melting in tantalum crucibles. The reaction mixtures were rapidly heated under argon to 1400 °C, cooled to 700 °C and kept at that temperature for another 2 h. For crystal growth, the elements were placed in tantalum crucibles and sealed in evacuated silica tubes. The latter were placed in a muffle furnace, rapidly annealed at 1050 °C and then cooled at a rate of 5 K/h to 750 °C. In a second step, these samples were cooled at a rate of 15 K/h to 450 °C and finally cooled within 5 h to room temperature.

Table 1
Lattice parameters (Guinier powder data) of the ternary indium compounds $RE_{14}Rh_3In_3$ (RE = Y, Dy–Tm, Lu)

Compound	a (pm)	c (pm)	V (nm^3)
$Y_{14}Rh_3In_3$	964.1(3)	2339(1)	2.1737
$Dy_{14}Rh_3In_3$	955.5(3)	2318.6(7)	2.1167
$Ho_{14}Rh_3In_3$	952.5(2)	2309.5(8)	2.0952
$Er_{14}Rh_3In_3$	948.0(3)	2301(1)	2.0676
$Tm_{14}Rh_3In_3$	941.7(4)	2287(1)	2.0276
$Lu_{14}Rh_3In_3$	937.5(2)	2277.7(6)	2.0020

2.2. X-ray powder data

The $RE_{14}Rh_3In_3$ samples were characterized through Guinier powder patterns using Cu$K\alpha_1$ radiation and α-quartz ($a = 491.30$, $c = 540.46$ pm) as an internal standard. The Guinier camera was equipped with an imaging plate system (Fujifilm, BAS-1800). The tetragonal lattice parameters (Table 1) were refined by least-squares calculations using the WinXPow software supplied by Stoe. To ensure correct indexing, the experimental patterns were compared with calculated ones [10], taking the atomic sites obtained from the structure refinements. As an example, we present an experimental and simulated powder pattern of $Y_{14}Rh_3In_3$ in Fig. 1. The powder diagrams have a characteristic pattern with an accumulation of stronger reflections around $2\theta = 34°$ and 57°.

2.3. Single-crystal X-ray diffraction

Irregularly shaped crystals of $RE_{14}Rh_3In_3$ (RE = Y, Dy, Ho, Er, Tm, Lu) were selected from the crushed arc-melted and annealed samples. These crystals were glued to small quartz fibres using a transparent varnish and first checked by Laue photographs on a Buerger camera, equipped with the same Fujifilm, BAS-1800 imaging plate technique. A good-quality crystal of each sample was used for the intensity data collection on a Stoe IPDS II diffractometer (graphite monochromatized Mo$K\alpha$ radiation; oscillation mode). Numerical absorption corrections were applied to the data sets. All relevant crystallographic data for the data collections and evaluations are listed in Tables 2 and 3.

2.4. Scanning electron microscopy

The single crystals investigated on the diffractometer were analyzed using a Leica 420 I scanning electron microscope with the *RE* trifluorides, Rh, and InAs as standards. No impurity elements heavier than sodium were observed. The compositions determined by EDX (70±2 at% Y : 15±2 at% Rh: 15±2 at% In, 60±3 at%

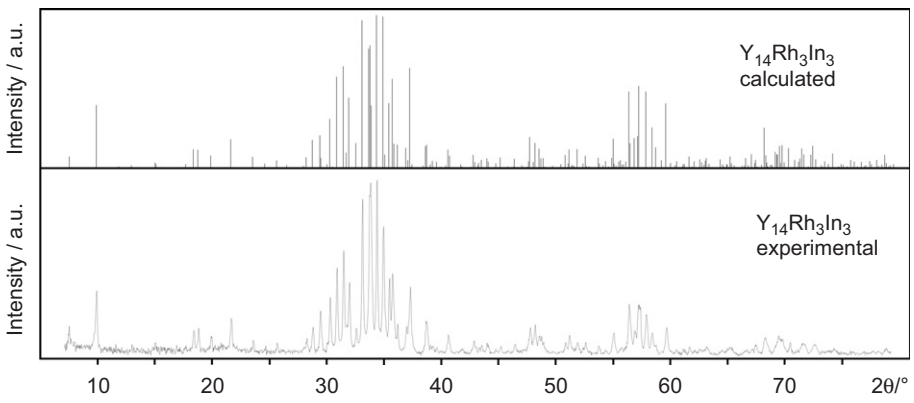

Fig. 1. Experimental and simulated Guinier powder diagram (Cu$K\alpha_1$ radiation) of $Y_{14}Rh_3In_3$.

Table 2
Crystal data and structure refinement for $Y_{14}Rh_3In_3$, $Dy_{14}Rh_{2.89(1)}In_3$, and $Ho_{14}Rh_{2.85(1)}In_3$, space group $P4_2/nmc$, $Z = 4$

Empirical formula	$Y_{14}Rh_3In_3$	$Dy_{14}Rh_{2.89(1)}In_3$	$Ho_{14}Rh_{2.85(1)}In_3$
Molar mass	1897.93 g/mol	2916.10 g/mol	2946.26 g/mol
Unit cell dimensions (single-crystal data)	$a = 961.7(1)$ pm	$a = 956.8(1)$ pm	$a = 952.4(1)$ pm
	$c = 2335.5(5)$ pm	$c = 2322.5(5)$ pm	$c = 2309.2(5)$ pm
	$V = 2.1560\,nm^3$	$V = 2.1262\,nm^3$	$V = 2.0946\,nm^3$
Calculated density	$5.84\,g/cm^3$	$9.11\,g/cm^3$	$9.34\,g/cm^3$
Crystal size	$10 \times 20 \times 140\,\mu m^3$	$10 \times 45 \times 65\,\mu m^3$	$20 \times 20 \times 90\,\mu m^3$
Detector distance	80 mm	80 mm	80 mm
Exposure time	11 min	8 min	5 min
ω Range; increment	0–180°; 1.0°	0–180°; 1.0°	0–180°; 1.0°
Integr. parameters A, B, EMS	14.0; 4.0; 0.013	13.5; 3.5; 0.012	12.6; 3.3; 0.010
Transmission ratio (max/min)	4.90	4.07	4.17
Absorption coefficient	$42.4\,mm^{-1}$	$53.8\,mm^{-1}$	$57.5\,mm^{-1}$
$F(000)$	3312	4803	4852
θ range	2–32°	2–30°	2–30°
Range in hkl	±14, ±13, ±34	±13, ±13, ±32	±13, ±13, ±32
Total no. reflections	23737	21293	20923
Independent reflections	2047 ($R_{int} = 0.104$)	1730 ($R_{int} = 0.138$)	1706 ($R_{int} = 0.080$)
Reflections with $I > 2\sigma(I)$	1142 ($R_\sigma = 0.115$)	1001 ($R_\sigma = 0.107$)	1129 ($R_\sigma = 0.064$)
Data/parameters	2047/62	1730/63	1706/63
Goodness-of-fit on F^2	0.640	0.720	0.711
Final R indices [$I > 2\sigma(I)$]	$R_1 = 0.029$	$R_1 = 0.032$	$R_1 = 0.023$
	$wR_2 = 0.047$	$wR_2 = 0.061$	$wR_2 = 0.039$
R indices (all data)	$R_1 = 0.072$	$R_1 = 0.075$	$R_1 = 0.048$
	$wR_2 = 0.052$	$wR_2 = 0.068$	$wR_2 = 0.041$
Extinction coefficient	0.00033(2)	0.00070(2)	0.000360(9)
Largest diff. peak and hole	$2.34/-1.66\,e/Å^3$	$3.12/-3.63\,e/Å^3$	$3.81/-2.47\,e/Å^3$

Table 3
Crystal data and structure refinement for $Er_{14}Rh_{2.86(1)}In_3$, $Tm_{14}Rh_{2.89(1)}In_3$, and $Lu_{14}Rh_{2.74(1)}In_3$, space group $P4_2/nmc$, $Z = 4$

Empirical formula	$Er_{14}Rh_{2.86(1)}In_3$	$Tm_{14}Rh_{2.89(1)}In_3$	$Lu_{14}Rh_{2.74(1)}In_3$
Molar mass	2980.17 g/mol	3007.15 g/mol	3076.53 g/mol
Unit cell dimensions (single-crystal data)	$a = 948.6(1)$ pm	$a = 943.8(1)$ pm	$a = 937.8(1)$ pm
	$c = 2302.8(5)$ pm	$c = 2291.5(5)$ pm	$c = 2276.5(5)$ pm
	$V = 2.0722\,nm^3$	$V = 2.0412\,nm^3$	$V = 2.0019\,nm^3$
Calculated density	$9.55\,g/cm^3$	$9.79\,g/cm^3$	$10.21\,g/cm^3$
Crystal size	$20 \times 20 \times 80\,\mu m^3$	$20 \times 70 \times 160\,\mu m^3$	$20 \times 40 \times 120\,\mu m^3$
Detector distance	80 mm	80 mm	80 mm
Exposure time	13 min	4 min	5 min
ω Range; increment	0–180°; 1.0°	0–180°; 1.0°	0–180°; 1.0°
Integr. parameters A, B, EMS	13.5; 3.5; 0.012	13.5; 3.5; 0.012	13.5; 3.5; 0.012
Transmission ratio (max/min)	5.17	6.44	4.94
Absorption coefficient	$61.4\,mm^{-1}$	$65.7\,mm^{-1}$	$73.8\,mm^{-1}$
$F(000)$	4910	4973	5058
θ range	2–32°	2–32°	2–30°
Range in hkl	±14, ±14, ±34	±14, ±14, ±34	±13, ±13, ±32
Total no. reflections	24003	23666	20041
Independent reflections	1977 ($R_{int} = 0.108$)	1936 ($R_{int} = 0.061$)	1637 ($R_{int} = 0.109$)
Reflections with $I > 2\sigma(I)$	1294 ($R_\sigma = 0.075$)	1473 ($R_\sigma = 0.036$)	1115 ($R_\sigma = 0.069$)
Data/parameters	1977/63	1936/63	1637/63
Goodness-of-fit on F^2	0.779	0.928	0.791
Final R indices [$I > 2\sigma(I)$]	$R_1 = 0.030$	$R_1 = 0.030$	$R_1 = 0.026$
	$wR_2 = 0.049$	$wR_2 = 0.062$	$wR_2 = 0.047$
R indices (all data)	$R_1 = 0.064$	$R_1 = 0.046$	$R_1 = 0.052$
	$wR_2 = 0.053$	$wR_2 = 0.065$	$wR_2 = 0.050$
Extinction coefficient	0.00074(2)	0.00035(2)	0.00135(3)
Largest diff. peak and hole	$2.34/-2.77\,e/Å^3$	$3.23/-3.01\,e/Å^3$	$2.64/-3.84\,e/Å^3$

Dy: 21±3 at% Rh: 19±3 at% In, 65±2 at% Ho: 18±2 at% Rh: 17±2 at% In, 72±2 at% Er: 14±2 at% Rh: 14±2 at% In, 65±2 at% Tm: 19±2 at% Rh: 16±2 at% In, 65±3 at% Lu: 20±3 at% Rh: 15±3 at% In) are close to the ideal composition, i.e. 70.0:15.0:15.0. The standard uncertainties account for the analyses at various points.

3. Results and discussion

3.1. Structure refinements

Analyses of the IPDS data sets revealed primitive tetragonal cells and the observed systematic extinctions were compatible with the centrosymmetric space group $P4_2/nmc$. Isotypy with the $Lu_{14}Co_3In_3$ [3] type was already evident from the X-ray powder data. The atomic parameters of $Y_{14}Co_3In_3$ [3] were taken as starting values and the structures were refined with anisotropic displacement parameters for all atoms with SHELXL-97 (full-matrix least-squares on F_o^2) [11]. Since the $RE_{14}Co_3In_3$ [2,3,12] and $RE_{14}Ni_3In_3$ [13] series revealed *RE*/In and *T*/In mixing on two 4*c* sites and cobalt defects on the 8*g* sites, the occupancy parameters have been refined in separate series of least-squares cycles. For the $RE_{14}Rh_3In_3$ series (except $Y_{14}Rh_3In_3$), we found only defects for the 8*g* Rh1 sites. These occupancy parameters have been refined as a least-squares variable in the final cycles, leading to the compositions listed in Table 4. Final difference Fourier syntheses revealed no significant residual peaks. The refinements then converged to the residuals listed in Tables 2 and 3 and the atomic parameters and interatomic

Table 4
Atomic coordinates and isotropic displacement parameters (pm^2) of $RE_{14}Rh_{3-x}In_3$ (*RE* = Y, Dy–Tm, Lu)

Atom	Wyckoff site	Occupancy (%)	*x*	*y*	*z*	U_{eq} [a]
$Y_{14}Rh_3In_3$						
Y1	4*c*	100	3/4	1/4	0.14594(6)	60(2)
Y2	4*d*	100	1/4	1/4	0.21561(6)	64(3)
Y3	8*g*	100	1/4	0.54925(12)	0.30689(4)	82(2)
Y4	8*g*	100	1/4	0.56151(12)	0.98379(4)	76(2)
Y5	8*f*	100	0.56170(8)	−*x*	1/4	88(2)
Y6	8*g*	100	1/4	0.44211(11)	0.46599(4)	67(2)
Y7	16*h*	100	0.43807(8)	0.43475(8)	0.10464(2)	64(1)
Rh1	8*g*	100	1/4	0.53116(9)	0.18916(3)	94(2)
Rh2	4*d*	100	1/4	1/4	0.55109(4)	80(2)
In1	4*c*	100	3/4	1/4	0.90937(4)	83(2)
In2	8*g*	100	1/4	0.41050(8)	0.85479(3)	65(1)
$Dy_{14}Rh_{2.89(1)}In_3$						
Dy1	4*c*	100	3/4	1/4	0.14588(7)	77(3)
Dy2	4*d*	100	1/4	1/4	0.21437(6)	60(3)
Dy3	8*g*	100	1/4	0.54762(12)	0.30710(5)	84(2)
Dy4	8*g*	100	1/4	0.56111(12)	0.98423(5)	80(2)
Dy5	8*f*	100	0.56282(8)	−*x*	1/4	81(2)
Dy6	8*g*	100	1/4	0.44391(12)	0.46593(5)	68(2)
Dy7	16*h*	100	0.44007(8)	0.43519(9)	0.10441(3)	60(2)
Rh1	8*g*	94(1)	1/4	0.5323(2)	0.18879(8)	82(7)
Rh2	4*d*	100	1/4	1/4	0.55139(11)	88(5)
In1	4*c*	100	3/4	1/4	0.90904(10)	110(4)
In2	8*g*	100	1/4	0.40933(15)	0.85477(8)	59(3)
$Ho_{14}Rh_{2.85(1)}In_3$						
Ho1	4*c*	100	3/4	1/4	0.14573(4)	88(2)
Ho2	4*d*	100	1/4	1/4	0.21451(4)	65(2)
Ho3	8*g*	100	1/4	0.54757(7)	0.30705(3)	91(1)
Ho4	8*g*	100	1/4	0.56139(7)	0.98412(3)	79(1)
Ho5	8*f*	100	0.56332(5)	−*x*	1/4	86(1)
Ho6	8*g*	100	1/4	0.44389(7)	0.46619(3)	73(1)
Ho7	16*h*	100	0.44034(5)	0.43484(5)	0.10451(2)	62(1)
Rh1	8*g*	92.3(6)	1/4	0.53236(13)	0.18897(5)	75(4)
Rh2	4*d*	100	1/4	1/4	0.55195(7)	84(3)
In1	4*c*	100	3/4	1/4	0.90913(6)	93(3)
In2	8*g*	100	1/4	0.40992(9)	0.85470(4)	64(2)
$Er_{14}Rh_{2.86(1)}In_3$						
Er1	4*c*	100	3/4	1/4	0.14569(5)	101(2)
Er2	4*d*	100	1/4	1/4	0.21471(4)	74(2)
Er3	8*g*	100	1/4	0.54782(8)	0.30747(3)	98(1)

Table 4 (*continued*)

Atom	Wyckoff site	Occupancy (%)	x	y	z	U_{eq} [a]
Er4	8*g*	100	1/4	0.56130(8)	0.98424(3)	85(1)
Er5	8*f*	100	0.56260(5)	$-x$	1/4	94(1)
Er6	8*g*	100	1/4	0.44405(8)	0.46612(3)	77(1)
Er7	16*h*	100	0.44047(5)	0.43495(6)	0.10440(2)	71(1)
Rh1	8*g*	92.8(8)	1/4	0.53163(14)	0.18914(6)	82(4)
Rh2	4*d*	100	1/4	1/4	0.55213(8)	84(3)
In1	4*c*	100	3/4	1/4	0.90960(7)	100(3)
In2	8*g*	100	1/4	0.40981(11)	0.85480(5)	65(2)
$Tm_{14}Rh_{2.89(1)}In_3$						
Tm1	4*c*	100	3/4	1/4	0.14563(3)	92(2)
Tm2	4*d*	100	1/4	1/4	0.21553(3)	71(2)
Tm3	8*g*	100	1/4	0.54946(7)	0.30909(3)	113(1)
Tm4	8*g*	100	1/4	0.56178(7)	0.98524(2)	85(1)
Tm5	8*f*	100	0.56098(5)	$-x$	1/4	90(1)
Tm6	8*g*	100	1/4	0.44506(7)	0.46546(2)	75(1)
Tm7	16*h*	100	0.43960(5)	0.43540(5)	0.10428(2)	66(1)
Rh1	8*g*	94.6(7)	1/4	0.53073(13)	0.19030(4)	92(4)
Rh2	4*d*	100	1/4	1/4	0.55139(6)	79(3)
In1	4*c*	100	3/4	1/4	0.91056(6)	115(3)
In2	8*g*	100	1/4	0.41057(10)	0.85534(4)	64(2)
$Lu_{14}Rh_{2.74(1)}In_3$						
Lu1	4*c*	100	3/4	1/4	0.14547(5)	84(2)
Lu2	4*d*	100	1/4	1/4	0.21422(4)	58(2)
Lu3	8*g*	100	1/4	0.54751(8)	0.30759(3)	87(2)
Lu4	8*g*	100	1/4	0.56068(8)	0.98444(3)	64(1)
Lu5	8*f*	100	0.56224(5)	$-x$	1/4	83(1)
Lu6	8*g*	100	1/4	0.44428(8)	0.46643(3)	57(1)
Lu7	16*h*	100	0.44086(6)	0.43532(6)	0.10438(2)	50(1)
Rh1	8*g*	87.2(8)	1/4	0.53202(17)	0.18958(7)	62(5)
Rh2	4*d*	100	1/4	1/4	0.55313(8)	61(3)
In1	4*c*	100	3/4	1/4	0.90955(7)	76(3)
In2	8*g*	100	1/4	0.41069(12)	0.85500(6)	55(2)

[a] U_{eq} is defined as one-third of the trace of the orthogonalized U_{ij} tensor.

distances listed in Tables 4 and 5. Further data on the structure refinements are available.[1]

3.2. Crystal chemistry

New indides $RE_{14}Rh_3In_3$ (RE = Y, Dy, Ho, Er, Tm, Lu) were synthesized by arc-melting or induction melting of the elements. They are new members of the tetragonal $Lu_{14}Co_3In_3$ type [2,3]. Similar to the $RE_{14}Co_3In_3$ [2,3,12] and $RE_{14}Ni_3In_3$ [13] series, also the $RE_{14}Rh_3In_3$ indides form only with the smaller RE elements. The cell volumes decrease from the dysprosium to the lutetium compound as expected from the lanthanoid contraction. The small deviations from a smooth curve are indicative for small homogeneity ranges, although only Rh1 defects were evident from the single-crystal data. Similar behavior has been observed in the $RE_{14}Co_3In_3$ [2,3,12] and $RE_{14}Ni_3In_3$ [13] series. Such small deviations in the cell volumes are frequently observed for compounds with homogeneity ranges. For all $RE_{14}T_3In_3$ series, no ytterbium-based indide was observed. Most likely ytterbium prefers the divalent oxidation state and the ytterbium atoms are too large to form such an indide.

The striking structural motifs are the rhodium-centred trigonal prisms formed by the RE atoms. In $Y_{14}Rh_3In_3$, the shortest interatomic distances occur for the Rh1–Y (276–286 pm) and Rh2–Y (271–284 pm) contacts. All of these distances are shorter than the sum of the covalent radii of 287 pm [14]. Thus, we observe strong rhodium–yttrium bonding. These RhY_6 prisms are condensed via common edges and corners, building two-dimensional frameworks (Fig. 2). Similar short distances occur also in the three-dimensional network of condensed $RhGd_6$ prisms in Gd_4RhIn (284 pm Gd–Rh) [4]. The space between the two-dimensional networks of trigonal prisms is filled by the polyhedra around the In1 and In2 atoms (Fig. 3 and 4).

[1] Details may be obtained from Fachinformationszentrum Karlsruhe, D-76344 Eggenstein-Leopoldshafen (Germany), by quoting the Registry Nos. CSD–417859 ($Y_{14}Rh_3In_3$), CSD–417862 ($Dy_{14}Rh_{2.89}In_3$), CSD–417863 ($Ho_{14}Rh_{2.85}In_3$), CSD–417864 ($Er_{14}Rh_{2.86}In_3$), CSD–417865 ($Tm_{14}Rh_{2.89}In_3$), CSD–417866 ($Lu_{14}Rh_{2.74}In_3$).

Table 5
Interatomic distances (pm), calculated with the single crystal lattice parameters of $Y_{14}Rh_3In_3$

Y1	2	In2	326.5	Y5	2	In2	337.4	Rh1	1	Y3	275.5
	4	Y5	353.1		2	Rh1	343.5		1	Y2	277.4
	2	Y4	353.1		2	Y3	344.8		2	Y7	283.3
	4	Y7	361.8		2	Y1	353.1		2	Y3	285.7
Y2	2	Rh1	277.4		2	Y2	359.3		1	In1	311.9
	2	Y3	358.2		2	Y7	359.7		2	Y5	343.5
	4	Y5	359.3		2	Y5	362.2	Rh2	2	Y6	271.4
	2	In2	359.8	Y6	1	Rh2	271.4		4	Y7	282.7
	4	Y7	362.6		1	In1	324.3		2	Y4	338.3
	1	Rh2	384.2		2	In2	354.1		1	Y2	384.2
Y3	1	Rh1	275.5		2	Y4	354.4	In1	2	Y3	307.5
	2	Rh1	285.7		2	Y7	363.9		2	Y4	308.4
	1	In1	307.5		2	Y4	366.5		2	Rh1	311.9
	2	Y5	344.8		2	Y7	369.4		2	Y6	324.3
	2	In2	345.2		1	Y6	369.5		4	Y7	354.5
	1	Y2	358.2		1	Y3	385.6	In2	1	In2	308.7
	2	Y7	367.1	Y7	1	Rh2	282.7		1	Y1	326.5
	2	Y3	381.0		1	Rh1	283.3		1	Y4	334.5
	1	Y6	385.6		1	In2	348.0		2	Y5	337.4
	1	Y3	386.1		1	In1	354.5		2	Y3	345.2
Y4	1	In1	308.4		1	Y7	355.4		2	Y7	348.0
	1	In2	334.5		1	Y4	356.7		2	Y6	354.1
	1	Rh2	338.3		1	Y5	359.7		1	Y2	359.9
	1	Y1	353.1		1	Y7	361.7				
	2	Y6	354.4		1	Y1	361.8				
	2	Y7	356.7		1	Y2	362.6				
	1	Y4	362.5		1	Y6	363.9				
	2	Y7	364.2		1	Y4	364.2				
	2	Y6	366.5		1	Y3	367.1				
					1	Y6	369.4				

All distances within the first coordination spheres are listed. Standard deviations are all equal or less than 0.2 pm.

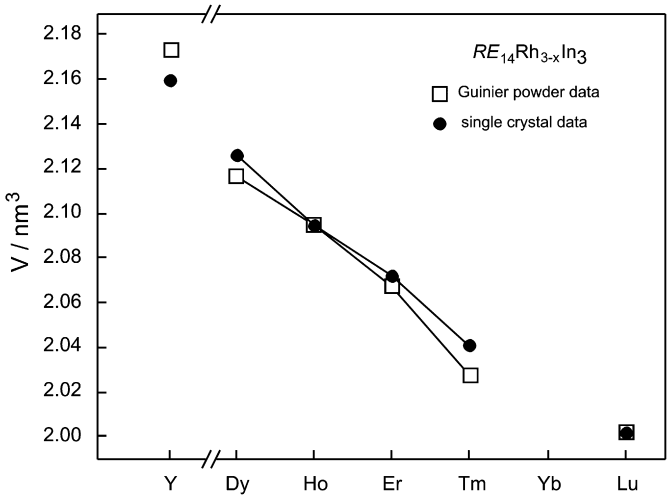

Fig. 2. Plot of the cell volumes of the tetragonal $RE_{14}Rh_{3-x}In_3$ indides.

Besides significant Rh–Y bonding we observe a broad range of Y–Y distances (345–386 pm) in this yttrium-rich compound. These distances compare well with the average Y–Y distance of 360 pm in *hcp* yttrium [15]. A similar range occurs for the Y–In distances (308–360 pm). The shorter

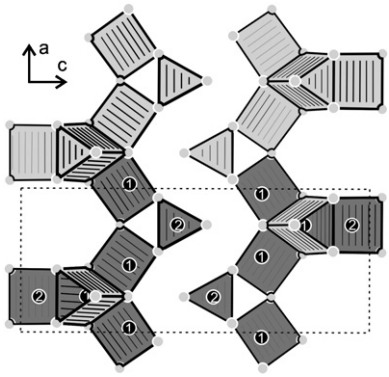

Fig. 3. Condensation of the Rh1RE_6 and Rh2RE_6 trigonal prisms in the structures of the $RE_{14}Rh_3In_3$ indides. For details see text.

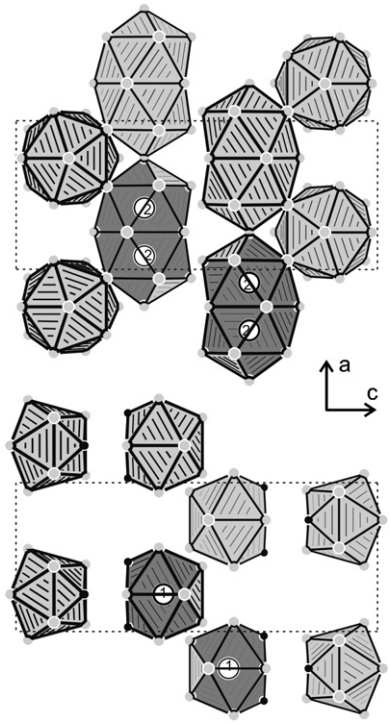

Fig. 4. View of the $RE_{14}Rh_3In_3$ structures along the *b*-axis. In the upper drawing, the condensation of the In2 coordination polyhedra is presented. The In1 polyhedra are drawn below. For details see text.

distances compare well with the sum of the covalent radii of 312 pm [14].

Although indium is the minority component in the $Y_{14}Rh_3In_3$ structure, we observe a segregation of the In2 atoms (Fig. 3). The latter have icosahedral coordination (11 Y + 1 In2) and always two of these icosahedra are interpenetrating, leading to dimeric units with short In2–In2 distances of 309 pm. These distances are much shorter than in tetragonal body-centered elemental indium (4×325 and 8×338 pm) [15]. In $Ho_{14}Co_{2.80}In_{2.89}$ [3], the In2–In2 distance of 300 pm is even shorter and we can safely assume strong In2–In2 bonding in these complex structures. For further details of the family of $RE_{14}T_3In_3$

indides we refer to our detailed crystal chemical description of the series $RE_{14}Co_3In_3$ [2,3] and $RE_{14}Ni_3In_3$ [13].

Finally we draw back to the occupancy parameters of the Rh1 site (Table 4). The lowest occupancy has been observed for the lutetium compound. Most likely the small size of lutetium is the reason for the lower occupancy. Such a trend has been observed in several other series of ternary rhodium-based indides, for details, see [16,17].

4. Conclusions

New $Lu_{14}Co_3In_3$ type *RE* metal-rich indides $RE_{14}Rh_{3-x}In_3$ ($RE = Y$, Dy, Ho, Er, Tm, Lu) have been synthesized from the elements by arc-melting or induction melting in tantalum crucibles. The structures are composed of two-dimensional networks of condensed trigonal prisms RE_6Rh. These networks are interconnected by the In1 and In2 atoms which both show distorted icosahedral coordination. The icosahedra around In2 are interpenetrating, leading to an indium segregation with In2–In2 pairs (309 pm in $Y_{14}Rh_3In_3$).

Acknowledgments

We are grateful to Dr. T. Nilges, Dr. R.-D. Hoffmann, and Dipl.-Ing. U.Ch. Rodewald for the intensity data collections and to Dipl.-Chem. F.M. Schappacher for the work at the scanning electron microscope. This work was supported by the Deutsche Forschungsgemeinschaft.

References

[1] Ya.M. Kalychak, V.I. Zaremba, R. Pöttgen, M. Lukachuk, R.-D. Hoffmann, Rare earth-transition metal-indides, in: K.A. Gschneidner Jr., V.K. Pecharsky, J.-C. Bünzli, Handbook on the Physics and Chemistry of Rare Earths, Elsevier, Amsterdam, vol., 34, 2005 (Chapter 218).
[2] V.I. Zaremba, Ya.M. Kalychak, P. Yu. Zavalii, Sov. Phys. Crystallogr. 37 (1992) 178.
[3] V.I. Zaremba, Ya.M. Kalychak, M.V. Dzevenko, U. Ch. Rodewald, B. Heying, R. Pöttgen, Z. Naturforsch. 61b (2006) 23.
[4] R. Zaremba, U.Ch. Rodewald, R.-D. Hoffmann, R. Pöttgen, Monatsh. Chem. 138 (2007) 523.
[5] Ya.V. Galadzhun, V.I. Zaremba, Ya.M. Kalychak, V.M. Davydov, A.P. Pikul, J. Stępień-Damm, D. Kaczorowski, J. Solid State Chem. 177 (2004) 17.
[6] Ya.M. Kalychak, V.I. Zaremba, J. Stępień-Damm, Ya.V. Galadzhun, L.G. Akselrud, Kristallografia 43 (1998) 17.
[7] R.E. Gladyshevsky, Yu.N. Grin, Ya.P. Yarmolyuk, Dopov. Akad. Nauk Ukr. RSR Ser. A 45 (1983) 67.
[8] M.V. Dzevenko, R.I. Zaremba, V.H. Hlukhyy, U.Ch. Rodewald, R. Pöttgen, Ya.M. Kalychak, Z. Anorg. Allg. Chem. 633 (2007) 724.
[9] R. Pöttgen, Th. Gulden, A. Simon, GIT Labor Fachzeitschrift 43 (1999) 133.
[10] K. Yvon, W. Jeitschko, E. Parthé, J. Appl. Crystallogr. 10 (1977) 73.
[11] G.M. Sheldrick, SHELXL-97, Program for Crystal Structure Refinement, University of Göttingen, Germany, 1997.
[12] F. Canepa, M. Napoletano, M.L. Fornasini, F. Merlo, J. Alloys Compd. 345 (2002) 42.
[13] M. Lukachuk, Ya.V. Galadzhun, R.I. Zaremba, M.V. Dzevenko, Ya.M. Kalychak, V.I. Zaremba, U. Ch. Rodewald, R. Pöttgen, J. Solid State Chem. 178 (2005) 2724.
[14] J. Emsley, The Elements, Oxford University Press, Oxford, 1999.
[15] J. Donohue, The Structures of the Elements, Wiley, New York, 1974.
[16] M. Lukachuk, U. Ch. Rodewald, V.I. Zaremba, R.-D. Hoffmann, R. Pöttgen, Z. Anorg. Allg. Chem. 630 (2004) 2253.
[17] M. Lukachuk, V.I. Zaremba, R.-D. Hoffmann, R. Pöttgen, Z. Naturforsch. 59b (2004) 182.